J. Fluid Mech. (2012), *vol.* 710, *pp.* 304–323.
doi:10.1017/jfm.2012.365

On Hadley flow in a porous layer with vertical heterogeneity

A. Barletta[1]† and D. A. Nield[2]

[1] DIENCA, Alma Mater Studiorum – Università di Bologna, Viale Risorgimento 2, I-40136 Bologna, Italy

[2] Department of Engineering Science, University of Auckland, Private Bag 92019, Auckland 1142, New Zealand

(Received 14 March 2012; revised 17 June 2012; accepted 17 July 2012; first published online 29 August 2012)

The onset of thermoconvective instability in a horizontal porous layer with a basic Hadley flow is studied, under the assumption of weak vertical heterogeneity. Hadley flow is a single-cell convective circulation induced by horizontal linear changes of the layer boundary temperatures. When combined with heating from below, these thermal boundary conditions yield a temperature gradient inclined to the vertical, in the basic state. The linear stability of the basic state is studied by considering small-amplitude disturbances of the velocity field and the temperature field. The linearized governing equations for the disturbances are then solved both by Galerkin's method of weighted residuals and by a combined use of the Runge–Kutta method and the shooting method. The effect of weak heterogeneity of the permeability and the effective thermal conductivity of the porous medium is studied with respect to neutral stability conditions. It is shown that, among the normal mode disturbances, the most unstable are longitudinal rolls, that is, plane waves with a wave vector perpendicular to the imposed horizontal temperature gradient. The effect of heterogeneity becomes important only for high values of the horizontal Rayleigh number, associated with the horizontal temperature gradient, approximately greater than 60. In this regime, the effect of heterogeneity is destabilizing. It is shown that heterogeneity with respect to thermal conductivity is of major importance in the onset of instability.

Key words: Bénard convection, buoyancy-driven instability, convection in porous media

1. Introduction

The analysis of instability in a horizontal fluid-saturated porous layer, where the basic state displays an inclined temperature gradient and a buoyant parallel flow with a vanishing mass flow rate, has been the subject of several investigations. This type of basic state is called Hadley flow, by analogy with the Hadley circulation named after George Hadley, an eighteenth-century meteorologist, who proposed an explanation for the distribution of winds in the atmosphere. The pioneering stability analysis of Hadley flow in a horizontal porous layer, modelled through Darcy's law, was carried out by Weber (1974). Weber's work was extended analytically by Nield (1990, 1991, 1998) and Nield, Manole & Lage (1993), and numerically by Manole & Lage (1995), and by

† Email address for correspondence: antonio.barletta@unibo.it

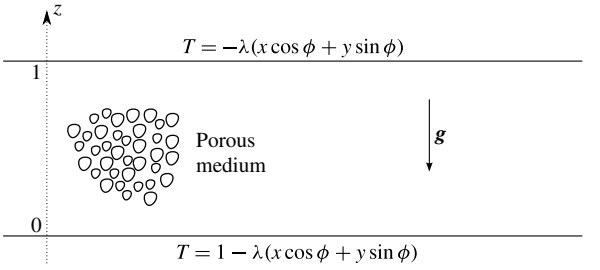

FIGURE 1. Drawing of the porous layer and the thermal boundary conditions.

Manole, Lage & Nield (1994) and Manole, Lage & Antohe (1995). Further extensions to the analysis have been made by a large number of people whose work has been surveyed in §§ 7.9 and 9.5 of Nield & Bejan (2006). More recent work has been reported by Narayana, Murthy & Gorla (2008), Brevdo & Ruderman (2009*a*,*b*) and Barletta & Nield (2010). To the best of the authors' knowledge, all the stability analyses of the Hadley flow in porous media to date were relative to homogeneous porous media.

In recent years increased attention has been directed to the effects of heterogeneity of the porous medium, and a considerable number of papers on this topic were surveyed by Nield (2008). In the case where heterogeneity is weak, a Rayleigh number based on averaged quantities serves as a useful criterion for stability, and an analytical solution can be obtained. A study of the effect of heterogeneity on the instability of a porous layer with a non-uniform wall temperature distribution was recently carried out by Barletta, Celli & Kuznetsov (2012).

The aim of this contribution is to investigate the effects of weak vertical heterogeneity of the porous medium on the stability of the Darcy–Hadley flow. We will assume that the permeability and thermal conductivity of the porous medium undergo a weak linear change in the vertical direction. The stability analysis will be carried out by considering linear perturbations of the basic state in the form of arbitrarily oriented oblique rolls. The linear stability theory that we apply is standard, but the problem is of interest because the permeability heterogeneity modifies the basic shear flow.

2. Governing equations

We consider a horizontal porous layer with thickness H and infinite horizontal width. We assume that the layer is bounded by a pair of impermeable plane walls with non-uniform temperatures changing linearly in the horizontal direction defined by the unit vector

$$\hat{\boldsymbol{s}} = \cos\phi\,\hat{\boldsymbol{e}}_x + \sin\phi\,\hat{\boldsymbol{e}}_y. \tag{2.1}$$

Here, $\hat{\boldsymbol{e}}_x$ and $\hat{\boldsymbol{e}}_y$ are unit vectors along the x-axis and the y-axis, respectively, and the angle $\phi \in [0, \pi/2]$ is arbitrary. A sketch of the porous layer is given in figure 1.

The forthcoming analysis is carried out under the following assumptions:

(i) Darcy's law is valid;

(ii) the Oberbeck–Boussinesq approximation with local thermal equilibrium between the solid phase and the fluid phase holds;

(iii) the porous medium is isotropic and displays weak vertical heterogeneity with variable dimensionless thermal conductivity, $k(z)$, and variable dimensionless permeability, $K(z)$;

(iv) viscous dissipation is negligible.

On account of these assumptions, the governing equations (see, for instance, Nield & Kuznetsov 2007, 2011) can be written in a dimensionless form as

$$\boldsymbol{\nabla}\cdot\boldsymbol{u}=0, \tag{2.2a}$$

$$\boldsymbol{\nabla}\times\left[\frac{\boldsymbol{u}}{K(z)}\right]=R\,\boldsymbol{\nabla}\times\left(T\,\hat{\boldsymbol{e}}_z\right), \tag{2.2b}$$

$$\frac{\partial T}{\partial t}+(\boldsymbol{u}\cdot\boldsymbol{\nabla})\,T=k(z)\nabla^2 T. \tag{2.2c}$$

In the Appendix it is shown that the local energy balance equation (2.2*c*) is appropriate when the heterogeneity is due to a non-uniform porosity of the medium, with very different thermal conductivities of the solid and the fluid, and slightly different volumetric heat capacities of the two phases.

We mention that (2.2*b*) is obtained by evaluating the curl of the local momentum balance equation, that is, of Darcy's law. Equations (2.2) are completed by the boundary conditions

$$z=0:\quad w=0,\quad T=1-\lambda\,(x\cos\phi+y\sin\phi)\,, \tag{2.3a}$$

$$z=1:\quad w=0,\quad T=-\lambda\,(x\cos\phi+y\sin\phi)\,. \tag{2.3b}$$

The dimensionless quantities are defined through the scaling

$$\frac{1}{H}\,(x^*,y^*,z^*)=(x,y,z)\,,\quad \frac{\alpha}{\sigma H^2}t^*=t,\quad \frac{H}{\alpha}\boldsymbol{u}^*=\frac{H}{\alpha}\,(u^*,v^*,w^*)=(u,v,w)=\boldsymbol{u}, \tag{2.4a}$$

$$\frac{T^*-T_0}{\Delta T}=T,\quad \frac{K^*(z^*)}{\langle K^*\rangle}=K(z),\quad \frac{k^*(z^*)}{\langle k^*\rangle}=k(z), \tag{2.4b}$$

where the asterisks denote the dimensional temperature and velocity fields $(T^*,\boldsymbol{u}^*)$, the dimensional coordinates and time (x^*,y^*,z^*,t^*), the dimensional permeability and thermal conductivity distributions (K^*,k^*). The average thermal conductivity over the vertical direction, $z^*\in[0,H]$, is denoted by $\langle k^*\rangle$. The average permeability over the vertical direction, $z^*\in[0,H]$, is denoted by $\langle K^*\rangle$. Thus, the average thermal diffusivity, α, is obtained dividing $\langle k^*\rangle$ by the volumetric heat capacity of the fluid. The ratio between the volumetric heat capacity of the fluid-saturated porous medium and that of the fluid is denoted by σ. The thermal expansion coefficient of the fluid is denoted by β, while g is the modulus of the gravitational acceleration $\boldsymbol{g}$, and ν is the kinematic viscosity of the fluid. The constant temperature difference between the walls at any fixed horizontal position, (x^*,y^*), is denoted by ΔT, while T_0 is a constant reference temperature.

In (2.2*b*), the Darcy–Rayleigh number R is defined by

$$R=\frac{g\beta\Delta T\langle K^*\rangle H}{\nu\alpha}, \tag{2.5}$$

while, in (2.3), the dimensionless parameter λ is the ratio between the magnitude of the prescribed horizontal temperature gradient and the constant $\Delta T/H$.

We note that, on account of (2.4), one obtains

$$\int_0^1 K(z)\,\mathrm{d}z = 1, \quad \int_0^1 k(z)\,\mathrm{d}z = 1. \tag{2.6}$$

3. Basic solution

A stationary solution of (2.2) and (2.3) describing a parallel horizontal throughflow with a vanishing mass flow rate can be found, given by

$$\boldsymbol{u}_b = \lambda R\,(z - c_1)\,K(z)\hat{\boldsymbol{s}}, \tag{3.1a}$$

$$T_b = 1 - \lambda\,(x\cos\phi + y\sin\phi) - c_2 z - \lambda^2 R \int_0^z \left\{ \int_0^\xi \left[\frac{K(\eta)}{k(\eta)}\,(\eta - c_1) \right] \mathrm{d}\eta \right\} \mathrm{d}\xi, \tag{3.1b}$$

where c_1 and c_2 are integration constants such that

$$c_1 = \int_0^1 \eta K(\eta)\,\mathrm{d}\eta, \quad c_2 = 1 - \lambda^2 R \int_0^1 \left\{ \int_0^\xi \left[\frac{K(\eta)}{k(\eta)}\,(\eta - c_1) \right] \mathrm{d}\eta \right\} \mathrm{d}\xi. \tag{3.2}$$

According to a hypothesis of weak heterogeneity (see, for instance, Nield & Kuznetsov 2007, 2011), we assume that both the permeability and the thermal conductivity are linear functions of z, such that

$$K(z) = 1 + \gamma_1\,(2z - 1)\,, \quad k(z) = 1 + \gamma_2\,(2z - 1)\,, \tag{3.3}$$

where γ_1 and γ_2 are assumed to be small, so that the integrals in (3.1) and (3.2) can be evaluated to first order in γ_1 and γ_2. Thus, the integration constants are given by

$$c_1 = \frac{1}{2} + \frac{\gamma_1}{6}, \quad c_2 = 1 + \frac{R\lambda^2}{12}\,(1 + \gamma_2)\,. \tag{3.4}$$

Equation (3.1) yields in this case

$$\boldsymbol{u}_b = \lambda R \left(z - \frac{1}{2} - \frac{\gamma_1}{6} \right) [1 + \gamma_1\,(2z - 1)]\,\hat{\boldsymbol{s}}, \tag{3.5a}$$

$$T_b = 1 - z - \lambda\,(x\cos\phi + y\sin\phi) - \frac{R\lambda^2}{12}[(1 + \gamma_2)z - (3 - 2\gamma_1 + 3\gamma_2)z^2 + 2(1 - 2\gamma_1 + 2\gamma_2)z^3 + 2(\gamma_1 - \gamma_2)z^4]. \tag{3.5b}$$

Equation (3.5), in the limits $\gamma_1 \to 0$ and $\gamma_2 \to 0$, coincides with the basic solution for the Hadley flow in a homogeneous porous medium reported in § 7.9 of Nield & Bejan (2006).

4. Linear stability

The linear perturbations to the basic solution are defined by

$$\boldsymbol{u} = \boldsymbol{u}_b + \varepsilon \boldsymbol{U}, \quad T = T_b + \varepsilon\theta, \tag{4.1}$$

where $\boldsymbol{U} = (U, V, W)$ and ε is a very small perturbation parameter.

If we substitute (4.1) into (2.2) and neglect the terms $O(\varepsilon^2)$, we obtain

$$\boldsymbol{\nabla}\cdot\boldsymbol{U} = 0, \tag{4.2a}$$

$$\boldsymbol{\nabla}\times\boldsymbol{U} = RK(z)\ \boldsymbol{\nabla}\times\left(\theta\hat{\boldsymbol{e}}_z\right), \tag{4.2b}$$

$$\frac{\partial\theta}{\partial t} + (\boldsymbol{u}_b\cdot\boldsymbol{\nabla})\,\theta + (\boldsymbol{U}\cdot\boldsymbol{\nabla})\,T_b = k(z)\nabla^2\theta. \tag{4.2c}$$

We note that, according to the assumption of weak heterogeneity, we approximated the term $\boldsymbol{\nabla}\times[\boldsymbol{U}/K(z)]$ with $(\boldsymbol{\nabla}\times\boldsymbol{U})/K(z)$ (see Nield & Kuznetsov 2007). From (2.3), (3.1) and (4.1), we obtain the boundary conditions

$$z=0,1: \quad W=0, \quad \theta=0. \tag{4.3}$$

Having considered a basic Hadley flow in a horizontal direction inclined to the x-axis, defined by the unit vector $\hat{\boldsymbol{s}}$, we are allowed to model an arbitrary normal mode of perturbation as a wave directed along the x-axis and such that $V=0$, with both $\boldsymbol{U}$ and θ independent of y. In this case, we can define a streamfunction ψ such that

$$U(x,z,t)=\frac{\partial\psi(x,z,t)}{\partial z}, \quad W(x,z,t)=-\frac{\partial\psi(x,z,t)}{\partial x}. \tag{4.4}$$

Thus, (4.2) and (4.3) yield

$$\frac{\partial^2\psi}{\partial x^2}+\frac{\partial^2\psi}{\partial z^2}+RK(z)\,\frac{\partial\theta}{\partial x}=0, \tag{4.5a}$$

$$\frac{\partial\theta}{\partial t}+\lambda\left[RF(z)\,\frac{\partial\theta}{\partial x}-\frac{\partial\psi}{\partial z}\right]\cos\phi+\left[1+\frac{R\lambda^2}{12}\,G(z)\right]\frac{\partial\psi}{\partial x} =k(z)\left(\frac{\partial^2\theta}{\partial x^2}+\frac{\partial^2\theta}{\partial z^2}\right), \tag{4.5b}$$

with

$$z=0,1: \quad \psi=0, \quad \theta=0. \tag{4.6}$$

On account of (3.5), functions $F(z)$ and $G(z)$ are defined by

$$F(z)=\frac{\boldsymbol{u}_b\cdot\hat{\boldsymbol{s}}}{\lambda R}=\left(z-\frac{1}{2}-\frac{\gamma_1}{6}\right)[1+\gamma_1(2z-1)], \tag{4.7a}$$

$$G(z)=-\frac{12}{R\lambda^2}\left(\frac{\partial T_b}{\partial z}+1\right) =1+\gamma_2-2(3-2\gamma_1+3\gamma_2)z+6(1-2\gamma_1+2\gamma_2)z^2+8(\gamma_1-\gamma_2)z^3. \tag{4.7b}$$

We now consider the normal mode solutions expressed as

$$\psi(x,z,t)=\mathrm{Re}\left\{\mathrm{i}f(z)\mathrm{e}^{\mathrm{i}(ax-\omega t)}\right\}, \quad \theta(x,z,t)=\mathrm{Re}\left\{h(z)\mathrm{e}^{\mathrm{i}(ax-\omega t)}\right\}, \tag{4.8}$$

where Re stands for the real part of a complex expression, while a is the dimensionless wavenumber and ω is the dimensionless frequency. The complex parameter ω is considered real on studying the neutral stability. At neutral stability, $\omega=0$ for the stationary modes and $\omega\neq0$ for the oscillatory, or travelling, modes.

Substitution of (4.8) into (4.5) and (4.6) yields

$$f''-a^2f+aRK(z)h=0, \tag{4.9a}$$

$$k(z)\left(h''-a^2h\right)+\mathrm{i}\omega h-\mathrm{i}\lambda\left[aRF(z)\,h-f'\right]\cos\phi+a\left[1+\frac{R\lambda^2}{12}\,G(z)\right]f=0, \tag{4.9b}$$

$$z=0,1: \quad f=0, \quad h=0. \tag{4.9c}$$

5. Longitudinal rolls

We now study the special case of longitudinal rolls, that is, normal modes with $\phi=\pi/2$. We will focus our attention on stationary longitudinal rolls, such that $\omega=0$.

Thus, equations (4.9) simplify to

$$f'' - a^2 f + aRK(z)h = 0, \tag{5.1a}$$

$$k(z)\left(h'' - a^2 h\right) + a\left[1 + \frac{R\lambda^2}{12}\,G(z)\right] f = 0, \tag{5.1b}$$

$$z = 0, 1: \quad f = 0, \quad h = 0. \tag{5.1c}$$

We seek an approximate solution of (5.1) by using Galerkin's method of weighted residuals (Finlayson & Scriven 1966; Finlayson 1972). To order N, we express f and h as finite sums,

$$f(z) = \sum_{n=1}^{N} f_n \chi_n(z), \quad h(z) = \sum_{n=1}^{N} h_n \chi_n(z), \tag{5.2}$$

where $\chi_n(z)$ are test functions such that $\chi_n(0) = \chi_n(1) = 0$, chosen as the polynomials

$$\chi_n(z) = (n+1)\,(n+2)\left(z^n - z^{n+1}\right), \quad n = 1, 2, 3, \ldots, N. \tag{5.3}$$

We substitute (5.2) into the left-hand sides of (5.1*a*), (5.1*b*), so that we evaluate the residuals associated with these differential equations. The weighted average of these residuals over the interval $0 \leqslant z \leqslant 1$, with weight functions coincident with the test functions $\chi_n(z)$, yields an algebraic linear system,

$$\boldsymbol{M} \cdot \boldsymbol{X} = 0. \tag{5.4}$$

Here, $\boldsymbol{X}$ is the $2N$-dimensional vector of the coefficients

$$\boldsymbol{X} = (f_1, f_2, \ldots, f_N, h_1, h_2, \ldots, h_N)\,, \tag{5.5}$$

$\boldsymbol{M}$ is the $2N \times 2N$ block matrix

$$\boldsymbol{M} = \begin{pmatrix} \boldsymbol{A} & \boldsymbol{B} \\ \boldsymbol{C} & \boldsymbol{D} \end{pmatrix}, \tag{5.6}$$

where, on account of (5.1), $\boldsymbol{A}$, $\boldsymbol{B}$, $\boldsymbol{C}$, $\boldsymbol{D}$ are the $N \times N$ matrices

$$A_{mn} = \int_0^1 \chi_m(z)\left[\chi_n''(z) - a^2\chi_n(z)\right] \mathrm{d}z, \tag{5.7a}$$

$$B_{mn} = aR \int_0^1 K(z)\chi_m(z)\chi_n(z)\,\mathrm{d}z, \tag{5.7b}$$

$$C_{mn} = a\int_0^1 \left[1 + \frac{R\lambda^2}{12}\,G(z)\right]\chi_m(z)\chi_n(z)\,\mathrm{d}z, \tag{5.7c}$$

$$D_{mn} = \int_0^1 k(z)\chi_m(z)\left[\chi_n''(z) - a^2\chi_n(z)\right]\mathrm{d}z, \quad m, n = 1, \ldots, N. \tag{5.7d}$$

Non-trivial solutions of (5.4) can exist only if

$$\det(\boldsymbol{M}) = 0. \tag{5.8}$$

For any choice of the input parameters $(a, \gamma_1, \gamma_2, \lambda)$, the solution of (5.8) allows one to obtain R. Following the literature (see, for instance, Nield & Bejan 2006), we prefer to introduce the horizontal Rayleigh number, R_H, defined by

$$R_H = R\lambda, \tag{5.9}$$

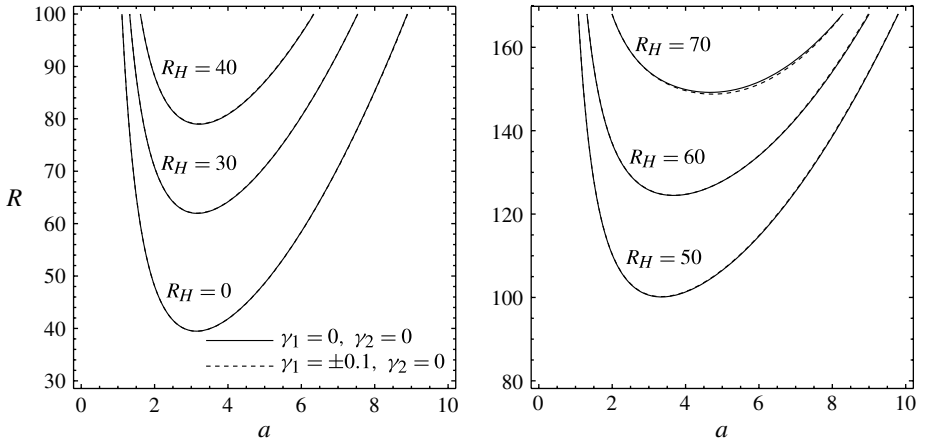

FIGURE 2. Longitudinal rolls: neutral stability curves $R(a)$ for different values of R_H. The solid lines are for the homogeneous case $\gamma_1 = \gamma_2 = 0$; the dashed lines are for the heterogeneous case $|\gamma_1| = 0.1$ and $\gamma_2 = 0$.

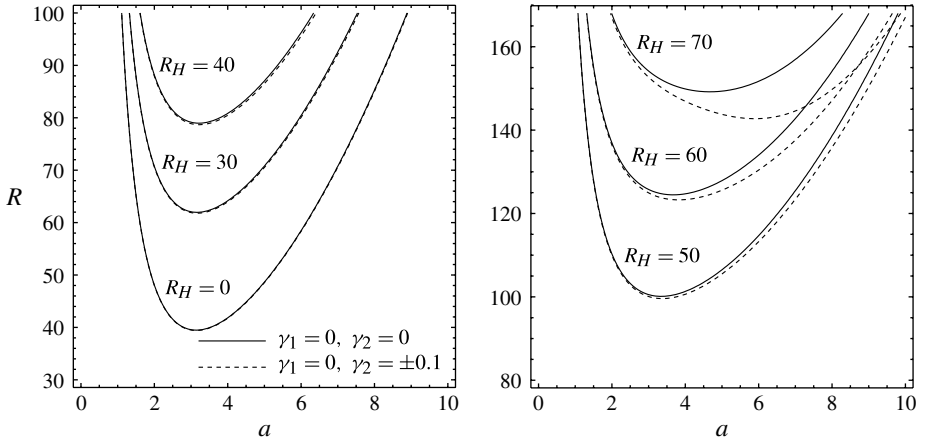

FIGURE 3. Longitudinal rolls: neutral stability curves $R(a)$ for different values of R_H. The solid lines are for the homogeneous case $\gamma_1 = \gamma_2 = 0$; the dashed lines are for the heterogeneous case $\gamma_1 = 0$ and $|\gamma_2| = 0.1$.

so that we may use (5.8) to obtain R for any set of input parameters $(a, \gamma_1, \gamma_2, R_H)$. This leads to the determination of the neutral stability curves $R(a)$ associated with each assigned set of parameters $(\gamma_1, \gamma_2, R_H)$. The absolute minima of these curves yield the critical values (a_c, R_c) for the onset of instability to longitudinal rolls.

Figures 2–5, obtained by the method of weighted residuals to order $N = 7$, display the neutral stability curves $R(a)$ for different values of R_H. Different possible cases of heterogeneity are considered in these figures. We gather a first important piece of information on the effects of the heterogeneity: the conductivity heterogeneity ($\gamma_2 \neq 0$) is more effective in changing the neutral stability conditions than the permeability heterogeneity ($\gamma_1 \neq 0$).

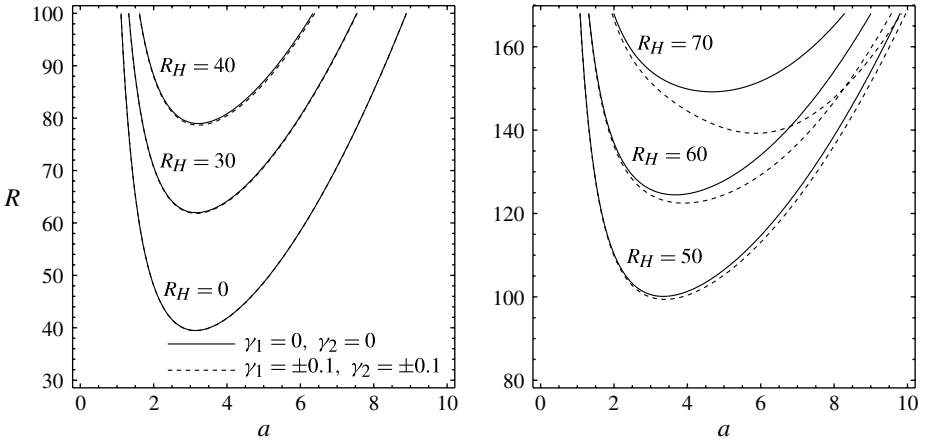

FIGURE 4. Longitudinal rolls: neutral stability curves $R(a)$ for different values of R_H. The solid lines are for the homogeneous case $\gamma_1 = \gamma_2 = 0$; the dashed lines are for the heterogeneous case $|\gamma_1| = |\gamma_2| = 0.1$ with $\gamma_1\gamma_2 > 0$.

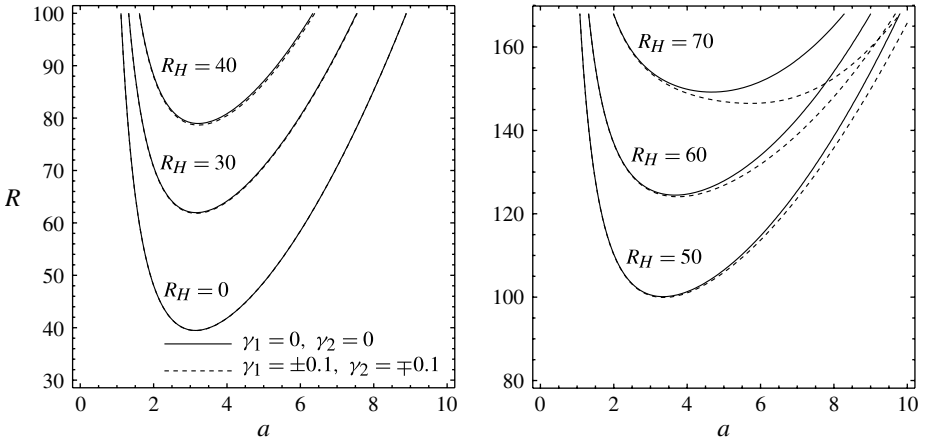

FIGURE 5. Longitudinal rolls: neutral stability curves $R(a)$ for different values of R_H. The solid lines are for the homogeneous case $\gamma_1 = \gamma_2 = 0$; the dashed lines are for the heterogeneous case $|\gamma_1| = |\gamma_2| = 0.1$ with $\gamma_1\gamma_2 < 0$.

We point out that the assumption of weak heterogeneity implies that the functions $K(z)$ and $k(z)$, given by (3.3), are invariant under the transformation

$$\gamma_1 \to -\gamma_1, \quad \gamma_2 \to -\gamma_2, \quad z \to 1 - z. \tag{5.10}$$

One can verify that functions F and G defined by (4.7), under the above transformation, behave as follows: $F \to -F$ and $G \to G$. Thus, the symmetry of the boundary conditions, (4.9*c*), implies that the neutral stability curve $R(a)$, obtained for general oblique rolls by solving (4.9), is left invariant by the transformation (5.10), provided that $\lambda \to -\lambda$. The latter change is physically insignificant as it can be balanced by an inversion of the horizontal axes x and y. This property of (4.9)

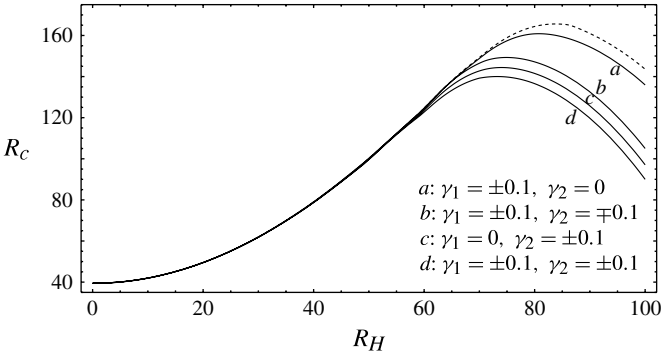

FIGURE 6. Longitudinal rolls: plots of R_c versus R_H for different heterogeneity models. The dashed line is for the homogeneous case ($\gamma_1 = \gamma_2 = 0$).

obviously holds also in the special case of longitudinal rolls, (5.1), where the sign of λ is immaterial as λ appears in (5.1) only with the power λ^2.

The discussion on the symmetry, (5.10), of the neutral stability condition justifies the assignment of two different weak heterogeneity models for each dashed curve in figures 2–5.

Tables 1 and 2 list the critical values of a and R for different assignments of R_H and of the heterogeneity parameters (γ_1, γ_2). We note that the values of a_c and R_c evaluated here for the homogeneous case ($\gamma_1 = \gamma_2 = 0$) are in perfect agreement, within six significant figures, with those reported by Kaloni & Qiao (1997) and by Barletta & Nield (2010). We point out a discrepancy with the results given in Barletta & Nield (2010) for $R_H = 90$, where the authors erroneously detected the minimum of the neutral stability curve for a higher mode. The results listed in table 1 are also in good agreement with those reported by Brevdo (2009) and by Diaz & Brevdo (2011) for $R_H \leqslant 60$. The effect of the heterogeneity is a change in a_c and R_c that yields either stabilization or destabilization of the flow. Whether R_c increases or decreases, relative to the homogeneous case, depends on the heterogeneity model, i.e. on the values assigned to γ_1 and γ_2, as well as on the value of R_H. The general behaviour for values of R_H larger than 60 is that heterogeneity implies destabilization of the basic Hadley flow. This conclusion is illustrated in figure 6, where R_c is plotted versus R_H for different heterogeneity models. The plot for the homogeneous case ($\gamma_1 = \gamma_2 = 0$) is reported, for comparison, as a dashed curve. We note that the strongest destabilization is caused by the heterogeneity model with ($\gamma_1 = \pm 0.1$, $\gamma_2 = \pm 0.1$).

6. Discussion of the mode selection

A rescaling of (4.9) using the transformation

$$f = R\tilde{f}, \quad h = \tilde{h}/a \tag{6.1}$$

produces the system

$$\tilde{f}'' - a^2\tilde{f} + K(z)\tilde{h} = 0, \tag{6.2a}$$

$$k(z)\left(\tilde{h}'' - a^2\tilde{h}\right) + \mathrm{i}\omega\tilde{h} - \mathrm{i}aR_H\cos\phi\left[F(z)\,\tilde{h} - \tilde{f}'\right] + a^2\left[R + \frac{R_H^2}{12}\,G(z)\right]\tilde{f} = 0, \tag{6.2b}$$

$$z = 0, 1: \quad \tilde{f} = 0, \quad \tilde{h} = 0. \tag{6.2c}$$

γ_1	γ_2	R_H	a_c	R_c
0	0	0	3.14159	39.4784
0	0	20	3.14575	49.5486
0	0	40	3.21522	78.9664
0	0	60	3.67219	124.473
0	0	70	4.67123	149.186
0	0	80	6.53124	164.371
0	0	90	7.73120	160.999
0	0	100	8.46277	143.586
±0.1	0	0	3.14215	39.4687
±0.1	0	20	3.14564	49.5630
±0.1	0	40	3.21389	79.0335
±0.1	0	60	3.67917	124.498
±0.1	0	70	4.73922	148.768
±0.1	0	80	6.56722	160.808
±0.1	0	90	7.49793	154.433
±0.1	0	100	8.24095	135.921
0	±0.1	0	3.14215	39.4169
0	±0.1	20	3.14725	49.4468
0	±0.1	40	3.22555	78.6818
0	±0.1	60	3.81735	123.269
0	±0.1	70	5.90324	142.740
0	±0.1	80	7.35681	141.527
0	±0.1	90	8.27177	125.759
0	±0.1	100	9.10612	97.0563

TABLE 1. Longitudinal rolls: critical values of a and R for different horizontal Rayleigh numbers and different heterogeneity data.

γ_1	γ_2	R_H	a_c	R_c
±0.1	±0.1	0	3.14109	39.4561
±0.1	±0.1	20	3.14523	49.4926
±0.1	±0.1	40	3.22508	78.6689
±0.1	±0.1	60	3.90483	122.491
±0.1	±0.1	70	5.86129	139.235
±0.1	±0.1	80	7.10281	136.569
±0.1	±0.1	90	7.96269	119.750
±0.1	±0.1	100	8.74954	89.9895
±0.1	∓0.1	0	3.14432	39.3584
±0.1	∓0.1	20	3.14904	49.4301
±0.1	∓0.1	40	3.22324	78.8299
±0.1	∓0.1	60	3.74213	124.087
±0.1	∓0.1	70	5.73015	146.479
±0.1	∓0.1	80	7.61748	147.153
±0.1	∓0.1	90	8.58748	132.548
±0.1	∓0.1	100	9.46843	105.019

TABLE 2. Longitudinal rolls: critical values of a and R for different horizontal Rayleigh numbers and different heterogeneity data.

It is now clear that the relevant parameters in the eigenvalue system are the vertical Rayleigh number R, the horizontal Rayleigh number R_H, the wavenumber a, and an 'orientation parameter' $aR_H\cos\phi$ (which has the value zero for longitudinal modes), as well as the heterogeneity parameters γ_1 and γ_2.

It is our belief that, for thermal instability of shear flows in a channel such as the present one, the favoured modes (the most unstable ones) are the stationary longitudinal ones. We do not have a formal proof for this. We cannot even prove that the 'principle of exchange of stabilities' (Chandrasekhar 1961, § 12) holds, since in fact (as we will see below) some oscillatory modes (transverse ones) grow with time. Nevertheless, we provide the following argument in support of our assertion. The basic ideas were introduced by Nield (1991).

In the case where the shear flow is not symmetric about the mid-plane of the channel, it is necessary to consider both even modes (symmetric about the mid-plane) and odd modes (anti-symmetric). (As is well known, any function of one variable can be expressed as the sum of an even function and an odd function.) The modes can be approximated by terms proportional to $\sin(n\pi z)$, where n is an integer. (Weak heterogeneity is not expected to change the eigenfunctions much.) The even modes correspond to odd integers. The most unstable even mode is given by $n=1$, and the most unstable odd mode by $n=2$.

The competition for favoured mode is between the following:

(i) stationary longitudinal modes;
(ii) stationary transverse modes;
(iii) oscillatory longitudinal modes;
(iv) oscillatory transverse modes.

The basic structure of the eigenvalue equation is given applying the Galerkin approximation at order two to the homogeneous case to (6.2*a*) and (6.2*b*). We now take as trial functions satisfying the boundary conditions (6.2*c*),

$$\chi_n(z)=\sin(n\pi z). \tag{6.3}$$

After some elementary row and column manipulations of the determinant, the eigenvalue equation takes the form

$$\det\begin{bmatrix} \pi^2+a^2 & 0 & 1 & 0 \\ 0 & 4\pi^2+a^2 & 0 & 1 \\ a^2\left(R-\dfrac{R_H^2}{4\pi^2}\right) & -\dfrac{8\mathrm{i}aR_H\cos\phi}{3} & \pi^2+a^2-\mathrm{i}\omega & \dfrac{-16\mathrm{i}aR_H\cos\phi}{9\pi^2} \\ \dfrac{8\mathrm{i}aR_H\cos\phi}{3} & a^2\left(R-\dfrac{R_H^2}{16\pi^2}\right) & \dfrac{-16\mathrm{i}aR_H\cos\phi}{9\pi^2} & 4\pi^2+a^2-\mathrm{i}\omega \end{bmatrix}=0. \tag{6.4}$$

Expanding the determinant and taking the real and imaginary parts gives the following pair of simultaneous equations:

$$\left(\tilde{R}-\tilde{R}_H^2-\frac{p^2}{4\tilde{a}^2}\right)\left(\tilde{R}-\frac{\tilde{R}_H^2}{4}-\frac{q^2}{4\tilde{a}^2}\right)+\frac{M\cos^2\phi\,\tilde{R}_H^2}{\tilde{a}^2}\left(pq+\frac{9}{4}\right)-\frac{pq\tilde{\omega}^2}{16\tilde{a}^4}=0, \tag{6.5a}$$

$$\tilde{\omega}\left(\tilde{R}-\frac{\tilde{R}_H^2(p+4q)}{4(p+q)}-\frac{pq}{4\tilde{a}^2}\right)=0. \tag{6.5b}$$

Here we have introduced the shorthand

$$\tilde{R} = \frac{R}{4\pi^2}, \quad \tilde{R}_H = \frac{R_H}{4\pi^2} = \frac{\lambda R}{4\pi^2}, \quad \tilde{a} = \frac{a}{\pi}, \quad \tilde{\omega} = \frac{\omega}{\pi^2}, \tag{6.6a}$$

$$p = 1 + \tilde{a}^2, \quad q = 4 + \tilde{a}^2, \quad M = \frac{256}{81\pi^2}. \tag{6.6b}$$

Stationary longitudinal modes ($\tilde{\omega} = 0,\ \phi = \pi/2$)

Equation (6.5*b*) is satisfied identically, and (6.5*a*) yields either

$$\tilde{R} = \tilde{R}_H^2 + \frac{(1+\tilde{a}^2)^2}{4\tilde{a}^2} \tag{6.7}$$

or

$$\tilde{R} = \frac{\tilde{R}_H^2}{4} + \frac{(4+\tilde{a}^2)^2}{4\tilde{a}^2}. \tag{6.8}$$

For the first mode, given by (6.7), the minimum value of $\tilde{R}$ is obtained when $\tilde{a} = 1$, and is given by

$$\tilde{R}_{LS1} = 1 + \tilde{R}_H^2, \tag{6.9}$$

where '*LS*' stands for 'longitudinal stationary'. Similarly, for the second mode the minimum value of $\tilde{R}$ is obtained when $\tilde{a} = 2$, and is given by

$$\tilde{R}_{LS2} = 4 + \tilde{R}_H^2/4. \tag{6.10}$$

We see that

$$\tilde{R}_{LS2} > \tilde{R}_{LS1} \quad \text{for } \tilde{R}_H < 2, \tag{6.11}$$

but

$$\tilde{R}_{LS2} < \tilde{R}_{LS1} \quad \text{for } \tilde{R}_H > 2. \tag{6.12}$$

Stationary transverse modes ($\tilde{\omega} = 0,\ \phi = 0$)

For this case (6.5*a*) gives

$$\left(\tilde{R} - \tilde{R}_H^2 - \frac{p^2}{4\tilde{a}^2}\right)\left(\tilde{R} - \frac{\tilde{R}_H^2}{4} - \frac{q^2}{4\tilde{a}^2}\right) + \frac{M\tilde{R}_H^2}{\tilde{a}^2}\left(pq + \frac{9}{4}\right) = 0. \tag{6.13}$$

Hence, for any stationary transverse mode the minimum, as $\tilde{a}$ varies, of the smaller root of this quadratic equation is applicable. It is found using some simple algebra that this minimum is greater than $\tilde{R}_{LS1}$ for $\tilde{R}_H < 2$, and greater than $\tilde{R}_{LS2}$ for $\tilde{R}_H \geqslant 2$.

Here, we have used $\tilde{R}_H = 2$ as the threshold value, due to its special role in marking the transition from the first stationary longitudinal mode to the second stationary longitudinal mode, pointed out above. Thus for any stationary transverse mode there is a more unstable longitudinal mode.

Oscillatory longitudinal modes ($\tilde{\omega} \neq 0,\ \phi = \pi/2$)

Now (6.5*b*) requires that

$$\tilde{R} = \frac{\tilde{R}_H^2(p+4q)}{4(p+q)} + \frac{pq}{4\tilde{a}^2}, \tag{6.14}$$

and this, together with (6.5*a*), requires that

$$\tilde{\omega}^2 = -9\left(1 - \frac{\tilde{R}_H^2\tilde{a}^2}{5+2\tilde{a}^2}\right)^2. \tag{6.15}$$

This gives no real value for $\tilde{\omega}$ and so there are no unstable oscillatory longitudinal modes.

Oscillatory transverse modes ($\tilde{\omega} \neq 0,\ \phi = 0$)

Again (6.14) applies, but in place of (6.15) we now have

$$\tilde{\omega}^2 = -9\left(1 - \frac{\tilde{R}_H^2\tilde{a}^2}{5+2\tilde{a}^2}\right)^2 + \frac{1024\tilde{R}_H^2\tilde{a}^2}{9\pi^2}\left[\frac{1}{(1+\tilde{a}^2)(4+\tilde{a}^2)} + \frac{4}{9}\right]. \tag{6.16}$$

It is only for values of $\tilde{R}_H$ exceeding a certain cut-off value that real values of $\tilde{\omega}$ are possible. For such values, it is necessary to return to (6.14) and minimize $\tilde{R}$ with respect to $\tilde{a}$ to obtain the critical value $\tilde{R}_{TO}$, the critical vertical Rayleigh number for transverse oscillatory disturbances which oscillate in time between a state with eigenfunction corresponding to the even mode ($n = 1$) and a state with eigenfunction corresponding to the odd mode ($n = 2$). Some further simple algebra indicates that $\tilde{R}_{TO}$ is always greater than $\tilde{R}_{LS1}$ given by (6.9) when $\tilde{R}_H < 2$, and greater than $\tilde{R}_{LS2}$ given by (6.10) when $\tilde{R}_H > 2$. Thus for any oscillatory transverse mode there is a more unstable longitudinal mode. The numerical results of Nield (1991) confirm this conclusion.

7. A numerical study of oblique rolls

An effective numerical strategy for solving the eigenvalue problem (4.9) is based on the combined use of the Runge–Kutta method and the shooting method. This procedure is discussed in § 9.1.1 of Straughan (2010) and can be efficiently implemented in the *Mathematica* 8.0 environment, as pointed out, for instance, in Barletta & Rees (2012).

We note that Galerkin's method of weighted residuals, employed in § 5 to solve the eigenvalue problem of linear stability for longitudinal rolls, can be extended to the case of oblique rolls. The procedure is qualitatively identical to that described in § 5, except for the matrix elements of $\boldsymbol{M}$ that, in the case of oblique rolls, are complex. The details are omitted here for the sake of brevity. We just mention that since for oblique rolls the matrix $\boldsymbol{M}$ is complex, (5.8) becomes a complex algebraic equation. On setting the real part of $\det(\boldsymbol{M})$ and the imaginary part of $\det(\boldsymbol{M})$ equal to zero, one obtains a system of two real algebraic equations which implicitly yield the neutral stability curve $R(a)$ and the dispersion relation $\omega(a)$. However, the solution method requires significantly long computational time to attain good accuracy. Therefore, we preferred to employ a Runge–Kutta solver combined with the shooting method, using the results obtained with Galerkin's method of weighted residuals as a first guess to initialize the shooting method. This solution strategy ensures that all branches of neutral stability are properly detected, and that very good numerical accuracy is achieved.

By adopting the combined Runge–Kutta method and shooting method, one can obtain the neutral stability function $R(a)$, as well as the dispersion relation $\omega(a)$, corresponding to the assigned input data $(\phi, R_H, \gamma_1, \gamma_2)$. On seeking the minimum of $R(a)$, one obtains the critical values (a_c, R_c) and the critical angular frequency

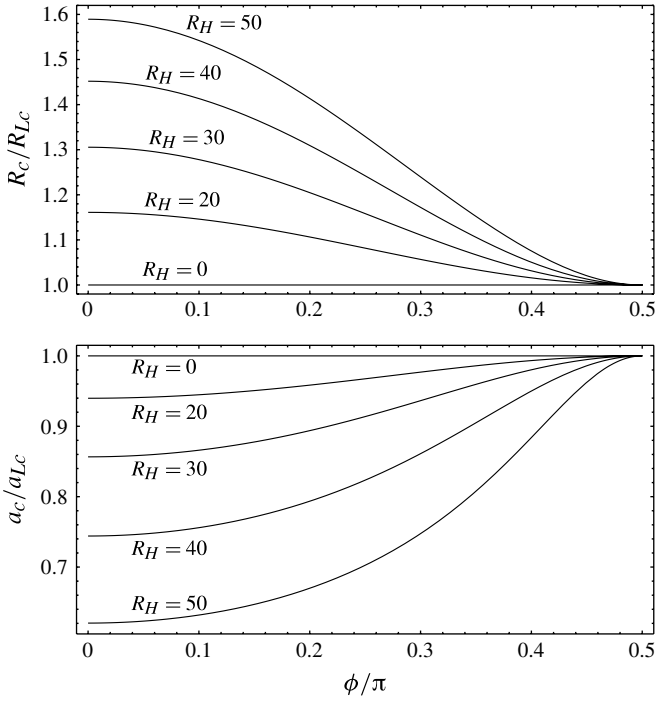

FIGURE 7. Oblique rolls: critical values of R and a for the homogeneous case $\gamma_1 = \gamma_2 = 0$, with different values of R_H.

$\omega_c = \omega(a_c)$. A test case of the methodology is the longitudinal rolls analysed in § 5. The numerical data reported in tables 1 and 2 agree, within all the reported figures, with those found by the procedure based on the combined Runge–Kutta method and shooting method. The latter numerical procedure allows one to analyse oblique rolls by tracking the change in the critical values (a_c, R_c, ω_c), while the inclination angle varies smoothly from $\phi = \pi/2$ (longitudinal rolls) to $\phi = 0$ (transverse rolls).

Figures 7–11 illustrate the change in the critical parameters (R_c, a_c, ω_c) with the inclination angle ϕ. For R_c and a_c, we displayed the values normalized to those for longitudinal rolls ($\phi = \pi/2$), denoted by R_{Lc} and a_{Lc}. The main differences arise on comparing the homogeneous case ($\gamma_1 = \gamma_2 = 0$), illustrated in figure 7, with the different models of heterogeneous porous media, illustrated in figures 8–11. In fact, for the homogeneous case, oblique rolls are non-oscillatory ($\omega_c = 0$), while for the heterogeneous cases oblique rolls are oscillatory ($\omega_c \neq 0$). The change in both R_c and a_c with ϕ is weakly affected by the heterogeneity model, while the trend of the critical angular frequency ω_c is markedly model-dependent. The horizontal Rayleigh number, R_H, plays an important role as it amplifies the effects of the inclination angle, i.e. the change in R_c, a_c and ω_c with ϕ. As illustrated in figures 7–11, the special case $R_H \to 0$, which implies boundary conditions of the Darcy–Bénard type, means that R_c, a_c and ω_c are independent of ϕ. This is expected, since in this limiting case the physics of the problem does not select any preferred horizontal direction, and hence there is no difference between the oblique and longitudinal rolls. An important feature, shown in figures 7–11, is that longitudinal rolls are the most unstable modes in all cases examined. This conclusion agrees with the analysis of the mode selection

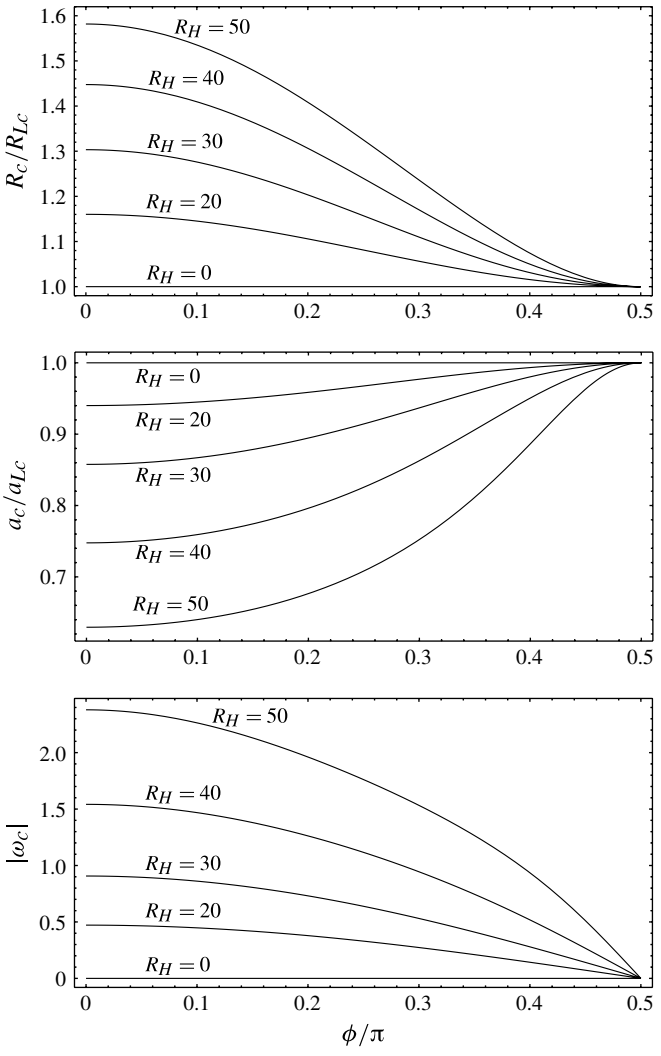

FIGURE 8. Oblique rolls: critical values of R and a for the heterogeneous case $|\gamma_1| = 0.1$ and $\gamma_2 = 0$, with different values of R_H. If $\gamma_1 > 0$ then $\omega_c \leqslant 0$; if $\gamma_1 < 0$ then $\omega_c \geqslant 0$.

reported in § 6. Therefore, the critical conditions for the onset of longitudinal rolls, described in § 5, are to be considered as the critical conditions for the basic solution to become linearly unstable.

8. Conclusions

The onset of thermal instability in a horizontal porous layer is studied, by considering a basic Hadley flow induced by linearly varying temperature distributions at the boundary walls, and by assuming a weak vertical heterogeneity of the porous medium. The governing dimensionless parameters of the heterogeneous Hadley flow are the permeability slope γ_1, the thermal conductivity slope γ_2, the horizontal Rayleigh number R_H, and the vertical Rayleigh number R. The stability of the basic flow has been tested by considering small-amplitude disturbances of the velocity field

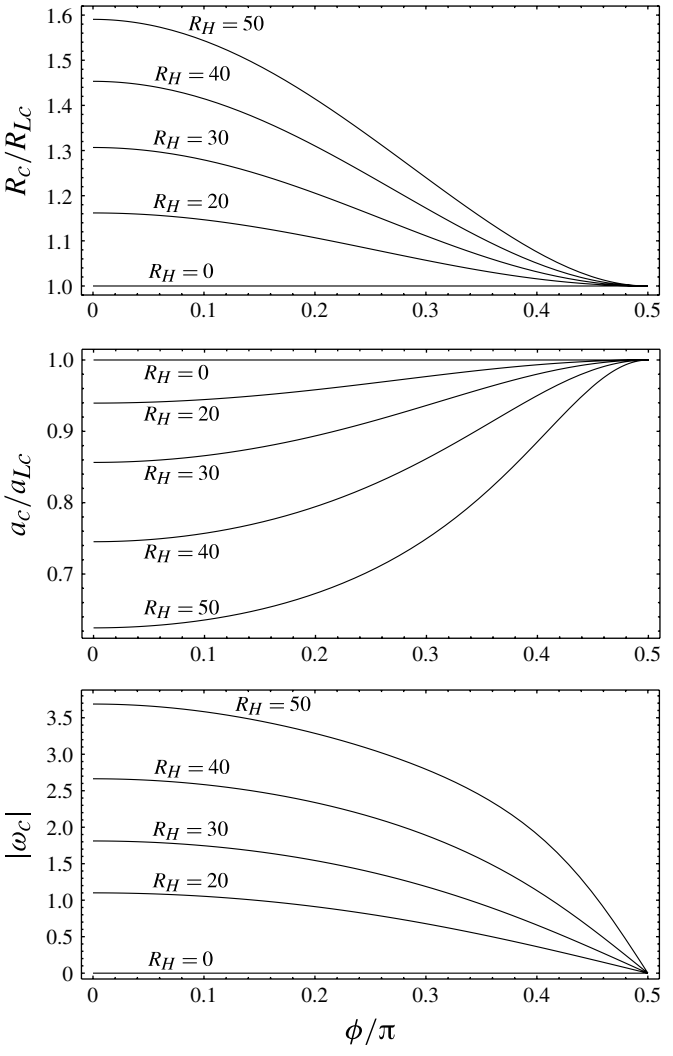

FIGURE 9. Oblique rolls: critical values of R and a for the heterogeneous case $\gamma_1 = 0$ and $|\gamma_2| = 0.1$, with different values of R_H. If $\gamma_2 > 0$ then $\omega_c \leqslant 0$; if $\gamma_2 < 0$ then $\omega_c \geqslant 0$.

and the temperature field. The standard normal mode analysis has been developed with respect to plane waves propagating along an arbitrary horizontal direction, with an inclination ϕ to the basic Hadley flow velocity. The neutral stability condition has been studied for longitudinal rolls, $\phi = \pi/2$, oblique rolls, $0 < \phi < \pi/2$, and transverse rolls, $\phi = 0$. The solution of the governing equations for the disturbances has been obtained both by a Galerkin method of weighted residuals, and by a numerical procedure based on the combined use of the Runge–Kutta method and the shooting method. The main results of the linear stability analysis are as follows.

(i) The analysis of the neutral stability condition for longitudinal rolls revealed that the heterogeneity of the porous medium is of minor importance for smaller values of R_H, approximately lower than 60. On the other hand, with larger values of R_H,

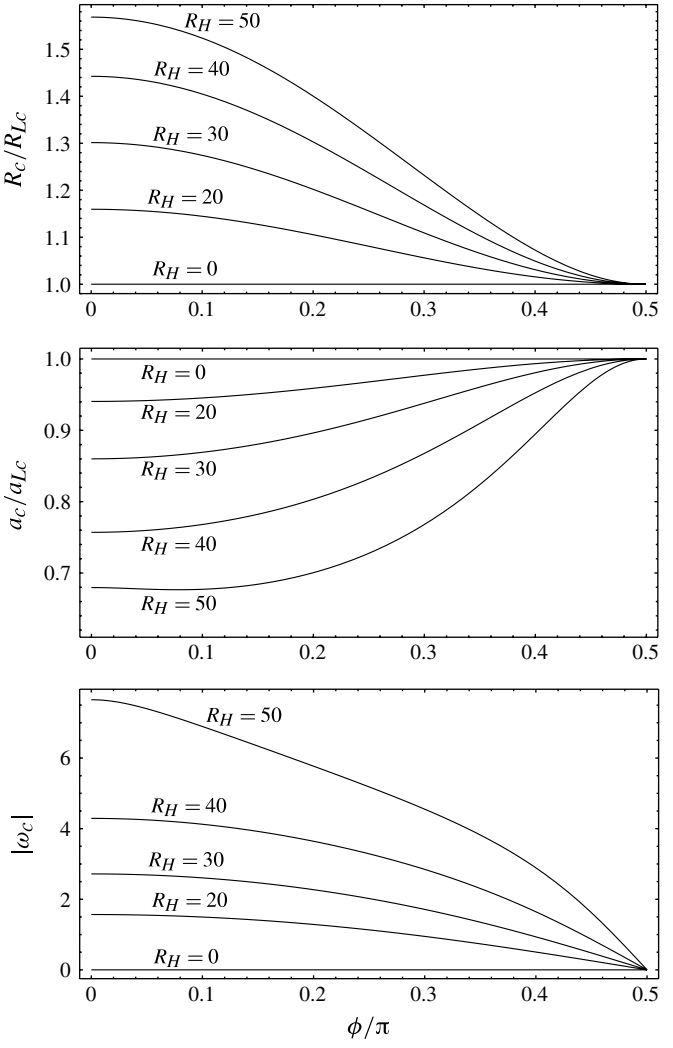

FIGURE 10. Oblique rolls: critical values of R and a for the heterogeneous case $|\gamma_1| = 0.1$ and $|\gamma_2| = 0.1$, $\gamma_1\gamma_2 > 0$, with different values of R_H. If $\gamma_1 > 0$ then $\omega_c \leqslant 0$; if $\gamma_1 < 0$ then $\omega_c \geqslant 0$.

the heterogeneity of the porous medium becomes more important and displays a destabilizing effect.

(ii) It has been proved that the non-homogeneous thermal conductivity ($\gamma_2 \neq 0$) yields a stronger change in the onset conditions for longitudinal rolls, if compared with the non-homogeneous permeability ($\gamma_1 \neq 0$). Among the tested cases, the heterogeneity model that yields the strongest discrepancy with respect to the homogeneous case is one with $\gamma_1\gamma_2 > 0$.

(iii) By adopting a second-order weighted residual solution relative to a homogeneous medium, it has been shown that no oscillatory longitudinal modes are allowed. Moreover, it has been pointed out that oscillatory or stationary transverse rolls may exist, but they are always more stable than stationary longitudinal rolls.

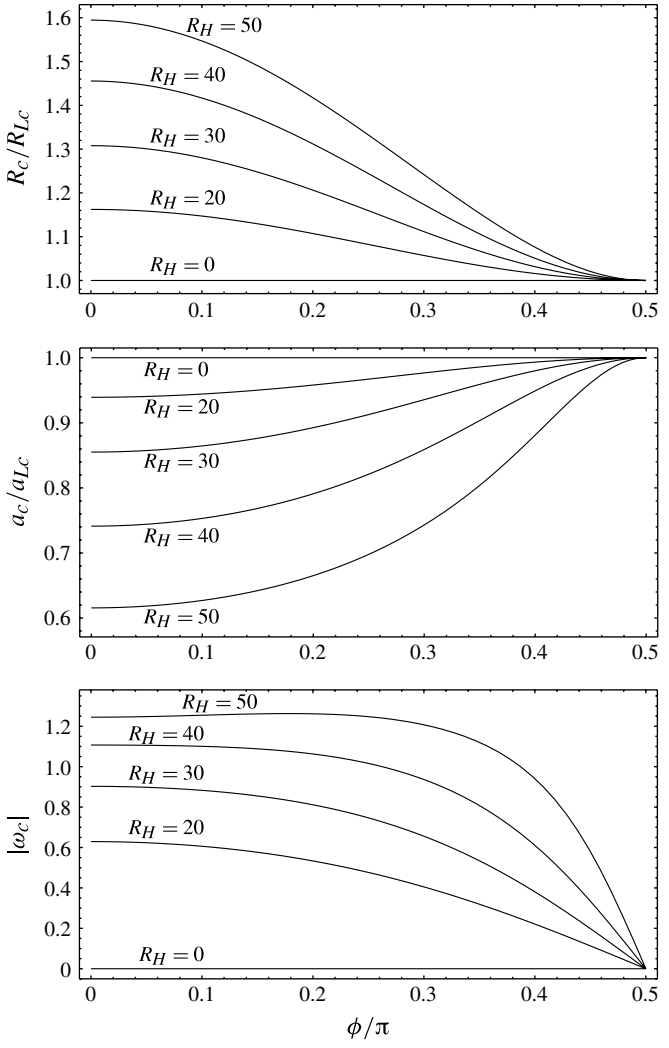

FIGURE 11. Oblique rolls: critical values of R and a for the heterogeneous case $|\gamma_1| = 0.1$ and $|\gamma_2| = 0.1$, $\gamma_1\gamma_2 < 0$, with different values of R_H. If $\gamma_2 > 0$ then $\omega_c \leqslant 0$; if $\gamma_2 < 0$ then $\omega_c \geqslant 0$.

(iv) The analysis of the mode selection has been extended to oblique rolls and to the general case of weak heterogeneity. This analysis has allowed us to prove that, on continuously varying the inclination angle ϕ from $\pi/2$ (longitudinal rolls) to 0 (transverse rolls), the critical value of R monotonically increases. This confirms the expected selection of stationary longitudinal rolls at the onset of instability.

Appendix

We consider a heterogeneous porous medium, such that the porosity φ, and hence the permeability K^*, vary along the vertical z^* direction. Thus we define two functions of the vertical coordinate, $\varphi(z^*)$ and $K^*(z^*)$. In this Appendix, the subscripts 's' and 'f' are used to denote the solid phase and the fluid phase, respectively. The

thermal properties of the solid phase and the fluid phase are considered to be uniform. In particular, the thermal conductivities, k_s and k_f, as well as the volumetric heat capacities, $(\rho c)_s$ and $(\rho c)_f$ (here, ρ is the density and c is the specific heat), are assumed to be uniform within the porous medium. This means that the heterogeneity has a morphological origin (variable porosity). Hence, the dimensional local energy balance equations for the fluid and for the solid can be written respectively as

$$[1-\varphi(z^*)]\,(\rho c)_s\,\frac{\partial T^*}{\partial t^*}=[1-\varphi(z^*)]k_s\nabla^{*2}T^*, \tag{A 1}$$

$$\varphi(z^*)\,(\rho c)_f\,\frac{\partial T^*}{\partial t^*}+(\rho c)_f\,\boldsymbol{u}^*\cdot\boldsymbol{\nabla}^*T^*=\varphi(z^*)k_f\nabla^{*2}T^*. \tag{A 2}$$

We mention that the length scale over which the heterogeneity described by $\varphi(z^*)$ is displayed is much larger than the local scale where the volume-averaging procedure (Nield & Bejan 2006) takes place.

When (A 1) and (A 2) are added together and divided by $(\rho c)_f$, we obtain

$$\frac{[1-\varphi(z^*)]\,(\rho c)_s+\varphi(z^*)\,(\rho c)_f}{(\rho c)_f}\,\frac{\partial T^*}{\partial t^*}+\boldsymbol{u}^*\cdot\boldsymbol{\nabla}^*T^*$$
$$=\frac{[1-\varphi(z^*)]k_s+\varphi(z^*)k_f}{(\rho c)_f}\nabla^{*2}T^*. \tag{A 3}$$

A special case is one where the thermal conductivities k_s and k_f greatly differ, so that we can define a variable effective conductivity

$$k^*(z^*)=\frac{[1-\varphi(z^*)]k_s+\varphi(z^*)k_f}{(\rho c)_f}, \tag{A 4}$$

while the volumetric heat capacities $(\rho c)_s$ and $(\rho c)_f$ slightly differ, so that we have an approximately constant heat capacity ratio

$$\sigma=\frac{[1-\varphi(z^*)]\,(\rho c)_s+\varphi(z^*)\,(\rho c)_f}{(\rho c)_f},\qquad \frac{\mathrm{d}\sigma}{\mathrm{d}z^*}\approx 0. \tag{A 5}$$

Equation (2.2*c*) is the dimensionless form of (A 3), under the assumptions expressed by (A 4) and (A 5).

REFERENCES

BARLETTA, A., CELLI, M. & KUZNETSOV, A. V. 2012 Heterogeneity and onset of instability in Darcy's flow with a prescribed horizontal temperature gradient. *Trans. ASME: J. Heat Transfer* **134**, 042602.

BARLETTA, A. & NIELD, D. A. 2010 Instability of Hadley–Prats flow with viscous heating in a horizontal porous layer. *Trans. Porous Med.* **84**, 241–256.

BARLETTA, A. & REES, D. A. S. 2012 Local thermal non-equilibrium effects in the Darcy–Bénard instability with isoflux boundary conditions. *Intl J. Heat Mass Transfer* **55**, 384–394.

BREVDO, L. 2009 Three-dimensional absolute and convective instabilities at the onset of convection in a porous medium with inclined temperature gradient and vertical throughflow. *J. Fluid Mech.* **641**, 475–487.

BREVDO, L. & RUDERMAN, M. 2009*a* On the convection in a porous medium with inclined temperature gradient and vertical throughflow. Part 1. Normal modes. *Trans. Porous Med.* **80**, 137–151.

BREVDO, L. & RUDERMAN, M. 2009*b* On the convection in a porous medium with inclined temperature gradient and vertical throughflow. Part 2. Absolute and convective instabilities, and spatially amplifying waves. *Trans. Porous Med.* **80**, 153–172.

CHANDRASEKHAR, S. 1961 *Hydrodynamic and Hydromagnetic Stability*. Dover.

DIAZ, E. & BREVDO, L. 2011 Absolute/convective instability dichotomy at the onset of convection in a porous layer with either horizontal or vertical solutal and inclined thermal gradients, and horizontal throughflow. *J. Fluid Mech.* **681**, 567–596.

FINLAYSON, B. A. 1972 *Method of Weighted Residuals and Variational Principles*. Academic.

FINLAYSON, B. A. & SCRIVEN, L. E. 1966 The method of weighted residuals: a review. *Appl. Mech. Rev.* **19**, 735–748.

KALONI, P. N. & QIAO, Z. 1997 Non-linear stability of convection in a porous medium with inclined temperature gradient. *Intl J. Heat Mass Transfer* **40**, 1611–1615.

MANOLE, D. M. & LAGE, J. L. 1995 Numerical simulation of supercritical Hadley circulation, within a porous layer, induced by inclined temperature gradients. *Intl J. Heat Mass Transfer* **38**, 2583–2593.

MANOLE, D. M., LAGE, J. L. & ANTOHE, B. V. 1995 Supercritical Hadley circulation within a layer of fluid saturated porous medium: bifurcation to traveling wave. *ASME HTD* **309**, 23–29.

MANOLE, D. M., LAGE, J. L. & NIELD, D. A. 1994 Convection induced by inclined thermal and solutal gradients, with horizontal mass flow, in a shallow horizontal layer of a porous medium. *Intl J. Heat Mass Transfer* **37**, 2047–2057.

NARAYANA, P. A. L., MURTHY, P. V. S. N. & GORLA, R. S. R. 2008 Soret-driven thermosolutal convection induced by inclined thermal and solutal gradients in a shallow horizontal layer of a porous medium. *J. Fluid Mech.* **612**, 1–19.

NIELD, D. A. 1990 Convection in a porous medium with inclined temperature gradient and horizontal mass flow. In *Heat Transfer 1990: Proceedings of the Ninth International Heat Transfer Conference, Jerusalem, Israel* (ed. G. Hetsroni), vol. 5, pp. 153–158. Hemisphere.

NIELD, D. A. 1991 Convection in a porous medium with inclined temperature gradient. *Intl J. Heat Mass Transfer* **34**, 87–92.

NIELD, D. A. 1998 Convection in a porous medium with inclined temperature gradient and vertical throughflow. *Intl J. Heat Mass Transfer* **41**, 241–243.

NIELD, D. A. 2008 General heterogeneity effects on the onset of convection in a porous medium. In *Emerging Topics in Heat and Mass Transfer in Porous Media* (ed. P. Vadász & J. Bear). *Theory and Applications of Transport in Porous Media*, vol. 22, pp. 63–84. Springer.

NIELD, D. A. & BEJAN, A. 2006 *Convection in Porous Media*, third edition. Springer.

NIELD, D. A. & KUZNETSOV, A. V. 2007 The effects of combined horizontal and vertical heterogeneity on the onset of convection in a porous medium. *Intl J. Heat Mass Transfer* **50**, 1909–1915.

NIELD, D. A. & KUZNETSOV, A. V. 2011 The effects of combined horizontal and vertical heterogeneity on the onset of convection in a porous medium with horizontal throughflow. *Intl J. Heat Mass Transfer* **54**, 5595–5601.

NIELD, D. A., MANOLE, D. M. & LAGE, J. L. 1993 Convection induced by inclined thermal and solutal gradients in a shallow horizontal layer of a porous medium. *J. Fluid Mech.* **257**, 559–574.

STRAUGHAN, B. 2010 *Stability and Wave Motion in Porous Media*. Springer.

WEBER, J. E. 1974 Convection in a porous medium with horizontal and vertical temperature gradients. *Intl J. Heat Mass Transfer* **17**, 241–248.